PHYSICAL REVIEW B **74**, 115320 (2006)

High-resolution core-level photoemission study of Eu-induced (3×2)/(3×4) reconstruction on Ge(111)

M. Kuzmin,* R. E. Perälä, P. Laukkanen, M. Ahola-Tuomi, and I. J. Väyrynen
Department of Physics, University of Turku, FIN-20014 Turku, Finland

(Received 26 April 2006; revised manuscript received 26 July 2006; published 22 September 2006)

We have investigated Eu-induced Ge(111)-$(3\times 2)/(3\times 4)$ reconstruction by high-resolution core-level photoelectron spectroscopy using synchrotron radiation and low-energy electron diffraction. Recent scanning tunneling microscopy (STM) observations [Phys. Rev. B **73**, 125332 (2006)] revealed that the Ge arrangement of this reconstruction can be well described in terms of the honeycomb chain-channel (HCC) geometry proposed earlier for metal/Si(111)-(3×1) and -(3×2) surfaces; the Eu atoms, however, were found to reside at two different adsorption sites in the Eu/Ge(111)-$(3\times 2)/(3\times 4)$ reconstruction, in contrast to the equivalent adsorption sites (e.g., *T*4) occupied in the case of Si. The present photoemission results provide further information about the atomic arrangement of Eu/Ge(111)-$(3\times 2)/(3\times 4)$. In particular, we show that the Ge 3*d* core-level data cannot be interpreted by the HCC structure with the Eu atoms adsorbed only on *T*4 sites, giving a spectroscopic support for the suggestions based on the earlier STM data. We consider here a modified HCC-based configuration for the Eu/Ge(111)-$(3\times 2)/(3\times 4)$ surface where the Eu atoms occupy two different sites in the empty channel between the neighboring Ge honeycomb chains. The atomic models are discussed in the context of the Ge 3*d* and Eu 4*f* data as well as the previous results available in the literature. Finally, we propose a structural model that allows us to account for the present photoemission and earlier STM findings.

DOI: 10.1103/PhysRevB.74.115320 PACS number(s): 68.35.−p, 68.43.Fg, 79.60.−i, 61.14.Hg

I. INTRODUCTION

Recently much attention has been drawn to nanoscale one-dimensional (1D) structures induced by the adsorption of metal atoms on Si surfaces because the increased electron correlation in these structures, which arises from the electron confinement by the reduced dimensionality, leads to a variety of exotic physical properties and phenomena such as Mott-Hubbard insulator,[1] non-Fermi-liquid ground state,[2] Peierls-like phase transition,[3] surface charge density wave,[3,4] spin-charge separation,[2,5] etc. In particular, interesting candidates for such 1D electron systems are considered to be the chainlike reconstructions induced by alkali metals (AM), alkaline-earth metals (AEM), and rare-earth metals (REM) on the Si(111) surface. The structural and electronic properties of these reconstructions have been the subject of various experimental and theoretical studies in the last years (e.g., Refs. 6–32 and references therein).

In contrast to the Si case, the chainlike structures induced by metal atoms on a Ge(111) surface have been less extensively studied to date.[8,33–40] Using scanning tunneling microscopy (STM) we have recently demonstrated (Ref. 40) that linear atomic chains, which arrange both the (3×2) and local (3×4) surface periodicities on Ge(111), can be stabilized by 1/6 monolayer (ML) of Eu [1 ML is referred to as the atomic density on the bulk-terminated (1×1) surface, i.e., 7.22×10^{14} atoms/cm^2 for Ge(111) and 7.84×10^{14} atoms/cm^2 for Si(111)]. The (3×2) and (3×4) phases were found to coexist on the Eu/Ge(111) surface at room temperature and to have similar Ge arrangements [for the sake of simplicity, we will refer to this surface showing the (3×2) and (3×4) periodicities as "Eu/Ge(111)-(3×2)" hereafter]. Moreover, the substrate arrangement of Eu/Ge(111)-(3×2) was revealed to be similar to those of the AM/Si(111)-(3×1) phases with a metal coverage of 1/3 ML, and the AEM/REM/Si(111)-(3×2) phases with a 1/6 ML coverage, for which the structural models constructed on the basis of the honeycomb chain-channel (HCC) geometry were widely adopted in recent years.[7–9,12,16–18,20–24,26–32] The atomic configurations of these 1/3 ML (3×1) and 1/6 ML (3×2) metal/Si phases are illustrated in Fig. 1. In the (3×1) phase [Fig. 1(a)], the metal atoms are proposed to reside at the *T*4 adsorption sites in the empty channels between the neighboring honeycomb chains formed by four topmost Si atoms *a*, *b*, *c*, and *d*. The (3×2) phase shown in Fig. 1(b) suggests the metal atoms to occupy half the *T*4 sites, while the other *T*4 sites remain unoccupied. Thus, both of the atomic structures in Fig. 1 imply that the metal atoms occupy the equivalent positions on the HCC Si backbone; for this reason, we

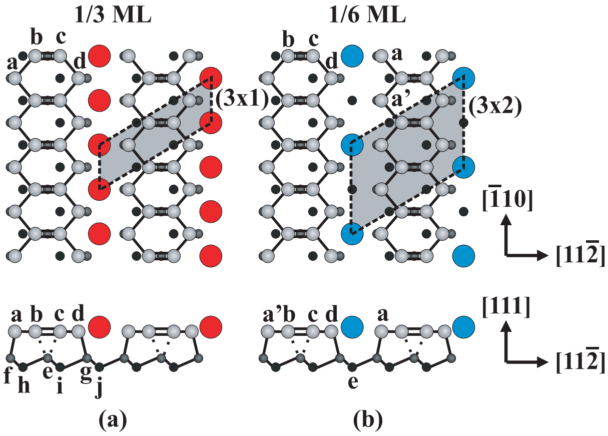

FIG. 1. (Color online) Atomic configurations of (a) the 1/3 ML (3×1) and (b) the 1/6 ML (3×2) reconstructions of metal/Si(111) surfaces. The metal atoms (large circles) are adsorbed on *T*4 sites in the empty channels of the HCC Si backbone. The (3×1) and (3×2) surface unit cells are marked.

will refer to such reconstructions as "T4" structures hereafter. The Eu/Ge(111)-(3×2) surface, however, reveals two different adsorption sites occupied by the metal atoms, as identified from the analysis of empty-state STM images of the (3×4) phase (Ref. 40). This phase is assumed to be a ground-state structure with two different positions of Eu atoms, whereas the (3×2) phase is proposed to originate from a dynamical fluctuation of Eu atoms between these sites.[40] However, complementary investigations are required to elucidate the atomic geometry and electronic structure of the Eu/Ge(111)-(3×2) surface.

In this study, we have utilized the high-resolution core-level photoelectron spectroscopy using synchrotron radiation to investigate the Eu $4f$ and Ge $3d$ line shapes of the Eu/Ge(111)-(3×2) surface. The core-level results are shown to be inconsistent with the $T4$ HCC model, in agreement with the previous STM measurements.[40] We propose an atomic model where the Eu atoms occupy two adsorption sites, with one of them being $T4$. The paper is organized as follows. In Sec. II, we briefly describe the experimental details. In Sec. III, we present the Eu $4f$ and Ge $3d$ photoemission data together with low-energy electron diffraction (LEED) observations for the Eu/Ge(111)-(3×2) surface. Finally, we discuss these results in the context of previous experimental and theoretical findings and atomic models available in the literature, and then propose a structural model of Eu/Ge(111)-(3×2) (Sec. IV).

II. EXPERIMENTAL

The experiments were performed on Beamline 33 at the MAX-lab national synchrotron radiation laboratory in Lund, Sweden. The Eu $4f$ and Ge $3d$ spectra were taken using an angle-resolved photoelectron spectrometer with an angular resolution of ~2°. The total energy resolution was ~200 meV in the Eu $4f$ measurements and better than 100 meV in the Ge $3d$ measurements. In all these measurements, the residual pressure was about 4×10^{-11} Torr. The binding energy (BE) was referred to the Fermi-level position of a metallic Ta sample in good electric contact with the Ge samples.

The Ge samples were cut from an Sb-doped (n-type) (111) wafer. Sample cleaning was carried out by repeated cycles of 1.0 keV Ar^+ sputtering at 673 K and subsequent annealing the sample at 900 K until an excellent $c(2\times8)$ LEED pattern with sharp fractional-order spots and a low background was displayed. A typical LEED pattern from the clean Ge(111) surface is shown in Fig. 2(a). The sample heating was performed by direct current. Temperature was measured by an infrared pyrometer. Europium was deposited from a W-filament evaporator. The Eu/Ge(111)-(3×2) surface was prepared by depositing Eu onto the clean substrate at 300 K, followed by annealing at 600 K for several minutes. The measurements were made at both 300 and 100 K.

III. RESULTS

A. LEED

LEED showed similar diffraction patterns for the Eu/Ge(111)-(3×2) at 300 and 100 K. Figure 2(b) gives a typical LEED pattern obtained at 100 K. It exhibits sharp (3×1) spots, which is a well-known indication of the (3×2) superstructure of divalent metal adsorbed Si(111)[13,16,18–20,25,27–30,41,42] and Ge(111) (Ref. 40) surfaces, where the (3×1) LEED periodicity can be associated with the geometry of the substrate. Also, it was previously shown that for AEM/ and REM/Si(111)-(3×2) reconstructions, the arrangement of the adsorbate subsystem can provide half-order LEED features (usually, faint ×2 streaks) found in some studies (e.g., Refs. 16, 18–20, 25, and 28–30). The intensity of these features depends on the degree of the metal chain correlation[31] and on the electron energy used in the LEED experiment (Ref. 29). In this study, neither ×2 nor ×4 LEED features were observed within detection limit. Thus we assume that the (3×1) LEED spots in Fig. 2(b) originate from the Ge arrangement of Eu/Ge(111)-(3×2), whereas the Eu overlayer of this surface does not give rise to any ordered LEED structure. In addition, we emphasize that no LEED spots from other surface structures, e.g., the $c(2\times8)$ spots of clean Ge(111), are found for the Eu/Ge(111) samples used in this study. Hence, the Eu $4f$ and Ge $3d$ spectra shown below are concluded to be contributed only by the Eu/Ge(111)-(3×2) reconstruction.

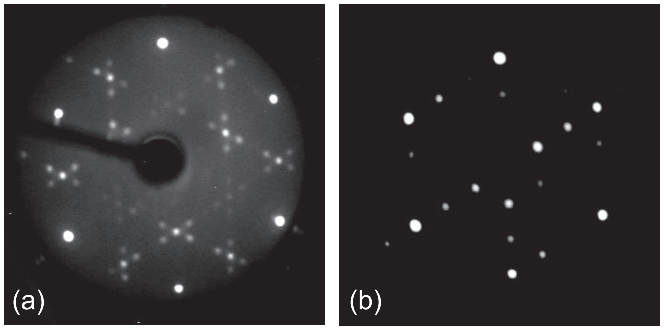

FIG. 2. LEED patterns of (a) the clean Ge(111)-$c(2\times8)$ surface at 300 K and (b) the Eu/Ge(111)-(3×2) surface at 100 K. The electron energy is (a) 40 eV and (b) 50 eV.

B. Eu 4f emission

The valence state of Eu atoms is very sensitive to the chemical surroundings of the atoms, and therefore, it can serve as an important criterion for structural models of the Eu/Ge(111) surface. The Eu valence can be determined from the Eu $4f$ spectrum where the $4f^6$ and $4f^5$ final-state features, which are due to the divalent (Eu^{2+}) and trivalent (Eu^{3+}) configurations respectively, are well resolved in energy.[43] Figure 3 shows Eu $4f$ spectra of Eu/Ge(111)-(3×2) taken at 300 and 100 K with the normal emission angle ($\theta_e=0°$) (open circles). To enhance the Eu $4f$ emission, the photon energy ($h\nu$) was chosen to be 142 eV, which corresponds to the maximum of $4d-4f$ resonance.[44] As seen, the peak at the BE of 2.25 eV is dominant in both the spectra. This feature is due to the $4f^6$ final state.[43] In contrast, no $4f^5$ final-state features, which can be expected in the BE range of ~6–8 eV,[45] are found in the spectra. We therefore conclude that the Eu atoms in the (3×2) reconstruction are divalent.

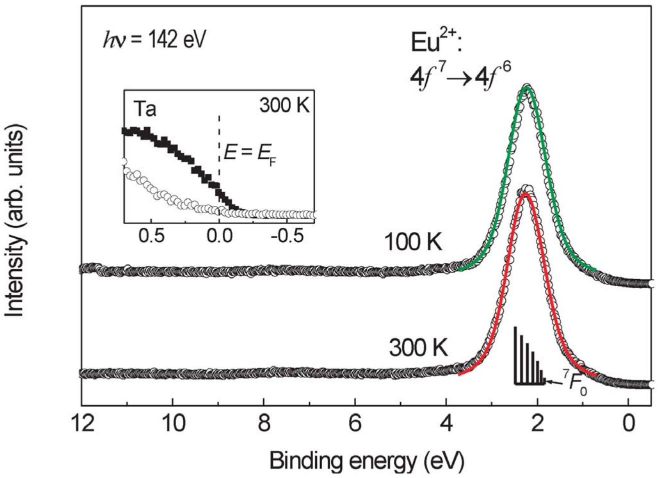

FIG. 3. (Color online) Eu 4f spectra from the Eu/Ge(111)-(3 × 2) surface at both 300 and 100 K. The photon energy is 142 eV. The open circles represent the experimental data. The solid bar diagram indicates the calculated intensities and binding energies for the ^7F_J (J=0,1,…,6) states of the divalent Eu atom. The solid lines, which reasonably fit the Eu^{2+} peaks, are obtained by convolution of these states. The inset illustrates the Eu 4f spectrum at 300 K in the BE range near E_F. For comparison, the valence-band spectrum of metallic Ta sample is shown.

For the divalent configuration of an Eu atom, there are seven possible final states for the excited 4f^6 ion, which are ^7F_J (J=0, 1, …, 6).[43] In Fig. 3, the solid bar diagram indicates the intensities and energy separations calculated for these seven levels, and the solid lines represent the multiplet structures, which are the convolutions of these levels. Such multiplet structures reasonably reproduce the experimental Eu^{2+} peaks, i.e., the Eu 4f^6 final-state emission from the Eu/Ge(111)-(3 × 2) surface can be well fitted by one component. Hence, we suggest that the Eu atoms at the Ge(111)-(3 × 2) surface have similar bonding configurations. At first glance, this result is inconsistent with the earlier STM observations that showed two adsorption sites for the Eu atoms in the (3 × 4) phase.[40] However, the photoemission and STM data can be reconciled by presuming that the (3 × 4) phase is a very local structure, and therefore, it does not contribute to the Eu 4f spectra significantly or/and the bonding configurations of Eu atoms in the (3 × 2) and (3 × 4) phases are very similar to each other. We also note in passing that the full width at half maximum of the Eu^{2+} peaks in Fig. 3 is very similar to those of the Eu/Si(111)-(3 × 2) surface where the Eu^{2+} emission was also fitted by a single ^7F_J (J =0, 1, …, 6) multiplet component.[30]

The inset of Fig. 3 shows in detail the Eu 4f spectrum at 300 K (open circles) in the BE range near the Fermi level (E_F). Comparing with the valence-band spectrum of the metallic Ta sample taken at $h\nu$=142 eV (solid squares), the Eu 4f spectrum is clearly seen to exhibit no emission near E_F. Thus the Eu/Ge(111)-(3 × 2) surface is semiconducting, in good agreement with previous scanning tunneling spectroscopy measurements.[40]

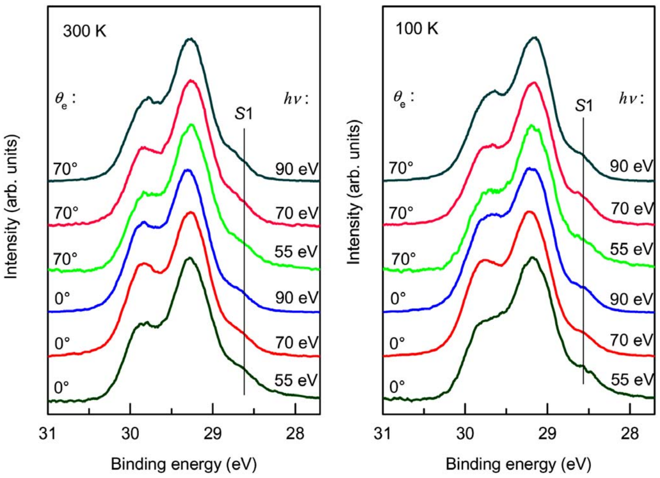

FIG. 4. (Color online) Ge 3d core-level spectra of Eu/Ge(111)-(3 × 2) taken at 300 K (left panel) and 100 K (right panel) with various photon energy ($h\nu$) and emission angle (θ_e).

C. Ge 3d core level

Figure 4 shows Ge 3d core-level spectra taken from the Eu/Ge(111)-(3 × 2) surface at 300 K (left panel) and 100 K (right panel) with various experimental conditions (i.e., $h\nu$ =55,70, and 90 eV, and θ_e=0 and 70°). Each spectrum was normalized to its maximum, and the background was removed by the Shirley's method. Without any fitting, it is clear that these spectra are contributed by the emission from the bulk and several nonequivalent surface Ge atoms. One of the surface components ($S1$) can be found at lower BE relative to the bulk component (B) because of the presence of a prominent shoulder at the BE of ~28.6 eV. Furthermore, another surface component(s) can be suggested by taking into account the asymmetrically broadened line shape of the Ge 3$d_{5/2}$ structure at the BE of ~29.25 eV as well as the shallow valley between this structure and the Ge 3$d_{3/2}$ structure at ~29.8 eV.

The Ge 3d core-level spectra from the Eu/Ge(111)-(3 × 2) surface were decomposed by using a standard least-squares-fitting procedure with a linear combination of spin-orbit split doublets consisting of Voigt functions. The values for spin-orbit splitting (0.58 eV), branching ratio (1.57), and Lorentzian width (LW=0.15 eV) parameters used throughout the fitting were extracted from the Ge 3d spectra of the clean Ge(111)-c(2 × 8) surface, which are thoroughly described in the literature.[46] Figure 5 illustrates the clean spectrum taken at 300 K with $h\nu$=83 eV and θ_e=0°. The reasonable fitting was obtained with the bulk component B and three surface-core-level-shifted (SCLS) components S_1', S_2', and S_3'. The Gaussian widths (GWs) of B and S_1'–S_3' were found to be 0.27 and 0.28–0.29 eV, respectively. The SCLSs obtained for S_1', S_2', and S_3' are −0.21, −0.70, and 0.19 eV, respectively, agreeing with the previous results.[46]

The spin-orbit splitting, branching ratio, and Lorentzian width obtained from the clean spectra (Fig. 5) were fixed for all experimental conditions ($h\nu$, θ_e, and T) while fitting the (3 × 2) spectra. The GWs were allowed to vary, reflecting small changes in the resolution with changing the photon

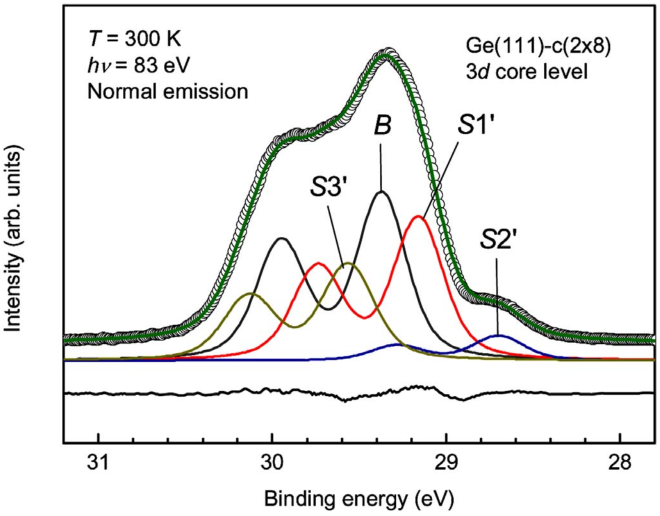

FIG. 5. (Color online) Ge 3d core-level spectrum of the clean Ge(111)-$c(2\times8)$ surface taken at 300 K with the photon energy of 83 eV and the normal emission angle. The raw data are shown by open circles. The decomposition of this spectrum is performed using one bulk component (B) and three surface components ($S1'-S3'$). The fitting parameters are given in the text. The resulting fitting curve is represented by a solid line. The residual between the experimental data and fitting curve is illustrated at the bottom of the spectrum.

energy. The SCLSs were also allowed to vary; however, they were assumed to be constant for each individual component in each series of spectra in Fig. 4. First we tried to fit the (3×2) spectra nominally using the bulk (B) and two surface doublets ($S1$ and $S2$). Such a fitting scheme was not found to be acceptable because the SCLSs and GWs of $S1$ and $S2$ were revealed to depend on $h\nu$ and θ_e. An introduction of a third surface component ($S3$) was enough to reproduce the spectra well, whereas the fourth surface component did not improve the fit. We therefore propose that the (3×2) spectra include the bulk component B and the three SCLS components $S1$, $S2$, and $S3$. Figure 6 shows the fitting results of the Ge 3d spectra of Eu/Ge(111)-(3×2) taken at 300 and 100 K with different surface sensitivities, i.e., $h\nu=55,70$, and 90 eV, and $\theta_e=0$ and 70°. The SCLSs of $S1$, $S2$, and $S3$ are -0.58 eV (-0.59 eV), -0.18 eV (-0.19 eV), and 0.14 eV (0.15 eV) at 300 K (100 K), respectively. The GWs of B are 0.262, 0.268, and 0.273 eV in the 300 K spectra and 0.238, 0.244, and 0.250 eV in the 100 K spectra at $h\nu=55,70$, and 90 eV, respectively. The GWs of $S1-S3$ are between 0.272 and 0.298 eV at 300 K, and between 0.249 and 0.275 eV at 100 K. The intensity ratios of $S1/B$, $S2/B$, and $S3/B$ increase by ∼15–30% at $h\nu=55$ eV, ∼20–40% at $h\nu=70$ eV, and ∼40–60% at $h\nu=90$ eV upon changing the emission angle θ_e from 0° to 70° (i.e., from more bulk-sensitive to more surface-sensitivity experimental conditions). Such behavior suggests the assignment of $S1-S3$ to the surface Ge bonding sites in the (3×2) reconstruction, which will be discussed in the following section.

IV. DISCUSSION

Since the earlier STM study showed that the Ge arrangement of the Eu/Ge(111)-(3×2) surface is well consistent with the HCC geometry,[40] we briefly consider previous Si 2p core-level results for the metal-induced Si(111)-(3×1) and -(3×2) reconstructions interpreted on the basis of the HCC structure. As depicted in Fig. 1, the HCC structure includes several nonequivalent substrate atoms in the top layer, e.g., the a and d atoms bonded to metal atoms directly, and the b and c atoms which form the double bond in the 1/3 ML (3×1) model [Fig. 1(a)]. Therefore, one can expect that such atomic configuration causes several SCLS components originating from the top atoms. In addition, core-level shifts can stem from the second- and third-layer atoms, i.e., the e, f, g, h, i, and j atoms in Fig. 1(a). In fact, the recent density-functional-theory calculations discovered a number of SCLSs for the (3×1) reconstruction induced by Li, Na, and K on Si(111).[12] However, most of these SCLSs caused by differences in the core-level binding energies of nonequivalent atoms were not resolved experimentally because of the limited instrumental resolution. In general, two surface components were resolved in the Si 2p spectra of AM/Si(111)-(3×1). The most evident one was found at the lower BE relative to the bulk peak.[12,47] This component was assigned to the both of the two outside atoms of the Si honeycomb chain, i.e., a and d in Fig. 1(a) (Refs. 9 and 12). The other surface component resolved at the higher BE relative to the bulk emission was assigned to the b and c atoms in Ref. 9 and several Si atoms (including b and c) in Ref. 12.

In contrast to the 1/3 ML (3×1) structure, the (3×2) structure with a 1/6 ML coverage has one metal atom per two (3×1) surface units. Within the $T4$ model [Fig. 1(b)], this leads to a difference in bonding configuration of substrate atoms on the right side of the honeycomb chain, i.e., the a and a' atoms. According to theoretical calculations and STM observations in Refs. 17, 18, 21, and 26, the Si honeycombs of the divalent metal adsorbed Si(111)-(3×2) surface are deformed, and this deformation is not equivalent for the neighboring honeycomb units. In particular, one honeycomb is more elongated in the [11-2] direction than the neighboring ones, and the lateral displacement perpendicular to the honeycomb chain is found to occur mostly at its left edge, which is formed by the atoms a and a' in the $T4$ model of Fig. 1(b). Thus the 1/6 ML (3×2) structure of the divalent metal adsorbed Si(111) surface is expected to result in different SCLSs for the outer honeycomb-chain atoms which are the d, a, and a' atoms within the $T4$ model [Fig. 1(b)]. Indeed, the recent Si 2p core-level measurements, performed for the Ca,[22,23] Ba,[20] and Eu (Refs. 29 and 30) induced (3×2) reconstructions on Si(111), revealed two SCLS components shifted to lower BE (typically, by ∼0.5 and ∼0.2–0.3 eV) and one SCLS component shifted to higher BE relative to B. Taking into account the intensity ratio and core-level binding energies of these surface components, the one with the lowest BE ($S1$) was assigned to the d atoms in Fig. 1(b), and the other component with the second lowest BE ($S2$) was interpreted as originating from the a atoms in Refs. 22, 29, and 30 and the a and a' atoms in Ref. 20. The third SCLS component at higher BE relative to B was attributed to the b, c, and/or e atoms.

In this study, the Ge 3d spectra of the Eu/Ge(111)-(3×2) surface also reveal three Ge 3d surface components: $S1$

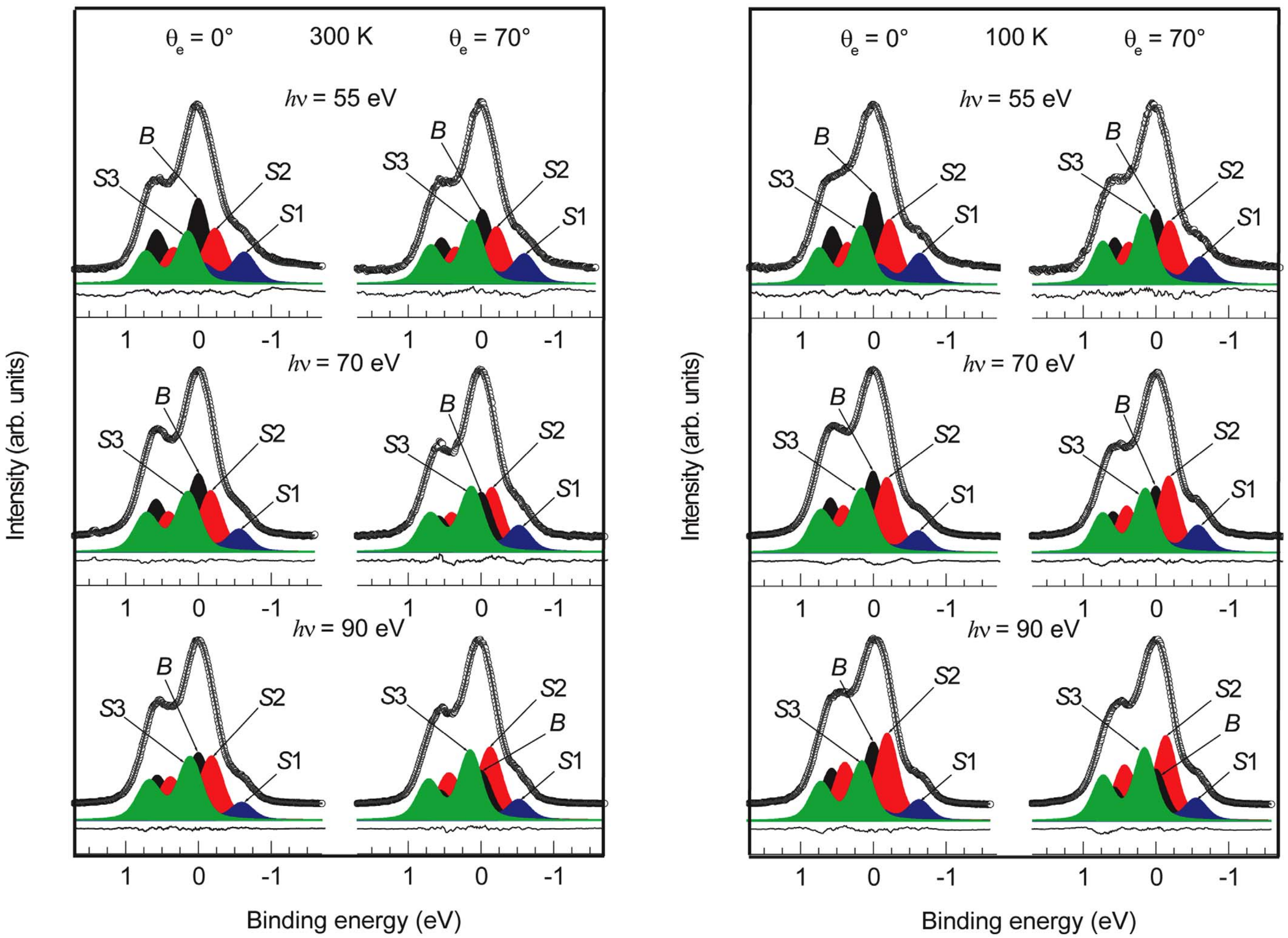

FIG. 6. (Color online) Decomposition of Ge 3*d* spectra from the Eu/Ge(111)-(3×2) surface. The experimental data are open circles. The fitting curves are shown by solid lines. Also indicated are the individual bulk (*B*) and surface (*S*1–*S*3) components. The binding energy is referenced to the bulk component. The residual between the experimental and fitting results is given at the bottom of each spectrum.

and *S*2 are shifted to lower BE and *S*3 to higher BE relative to *B* (Fig. 6). The number of these components and their core-level shifts are similar to those of the AEM/ and REM/Si(111)-(3×2) surfaces in Refs. 20, 22, 23, 29, and 30. However, the intensity ratio of *S*1 and *S*2 for Eu/Ge(111)-(3×2) differs dramatically from those of the AEM/ and REM/Si(111)-(3×2) surfaces. The present *S*1/*S*2 intensity ratio is about 1:2 at $h\nu$=55 eV, 1:3 at $h\nu$=70 eV, and 1:4 at $h\nu$=90 eV in Fig. 6. In contrast, it is about 1:1 at 300 K and varies between ~2:1 and 7:1 at 100 K for Ca/Si(111)-(3×2).[22,23] Also, the *S*1/*S*2 intensity ratio is ~2:1 for Eu/Si(111)[29,30] and ~1:1 for Ba/Si(111) (Ref. 20). Since the intensity ratio of *S*1 and *S*2 is assumed to reflect the number ratio of outer honeycomb-chain atoms that are bonded to the metal atoms, the Ge 3*d* core-level results obtained in this study cannot be interpreted within the *T*4 model of Fig. 1(b), which is proposed for the Ca/, Eu/, and Ba/Si(111)-(3×2) surfaces. We therefore conclude that the atomic arrangement of Eu/Ge(111)-(3×2) is different from the structure in Fig. 1(b).

We propose a modified HCC-based geometry for the Eu/Ge(111)-(3×2) surface, which allows us to explain reasonably the present photoemission data as well as the earlier STM data (Ref. 40). According to STM, the Eu-induced (3×2) and (3×4) phases have a similar Ge backbone that is consistent with the HCC arrangement. As remarked above, the (3×4) phase is proposed to be a ground state with two adsorption sites for the Eu atoms, whereas the (3×2) phase is suggested to originate from a dynamical fluctuation of Eu atoms between these two sites. Assuming that the Eu atoms occupy equally both adsorption sites in the (3×2) phase, we expect that the (3×4) and (3×2) structures cannot be distinguished in photoemission. In the Si(111)-(3×2) HCC structure, the favorable adsorption site for most of the AEM and REM adsorbates is found to be the *T*4 site in the channel between the neighboring honeycomb chains [except Mg for which *H*3 is slightly more stable than *T*4 (see Ref. 21)].[17,18,21,26,32] Therefore, the atomic models of the Eu/Ge(111)-(3×2) and -(3×4) phases can be constructed by placing half of the Eu atoms (i.e., 1/12 ML) at *T*4 sites and the rest of the Eu atoms (1/12 ML) at other sites. Among the other adsorption sites, the *H*3 one is almost as favorable as the *T*4 site in the HCC geometry.[18,32] Hence, we can propose *H*3 to be another Eu adsorption site in the Ge(111)-

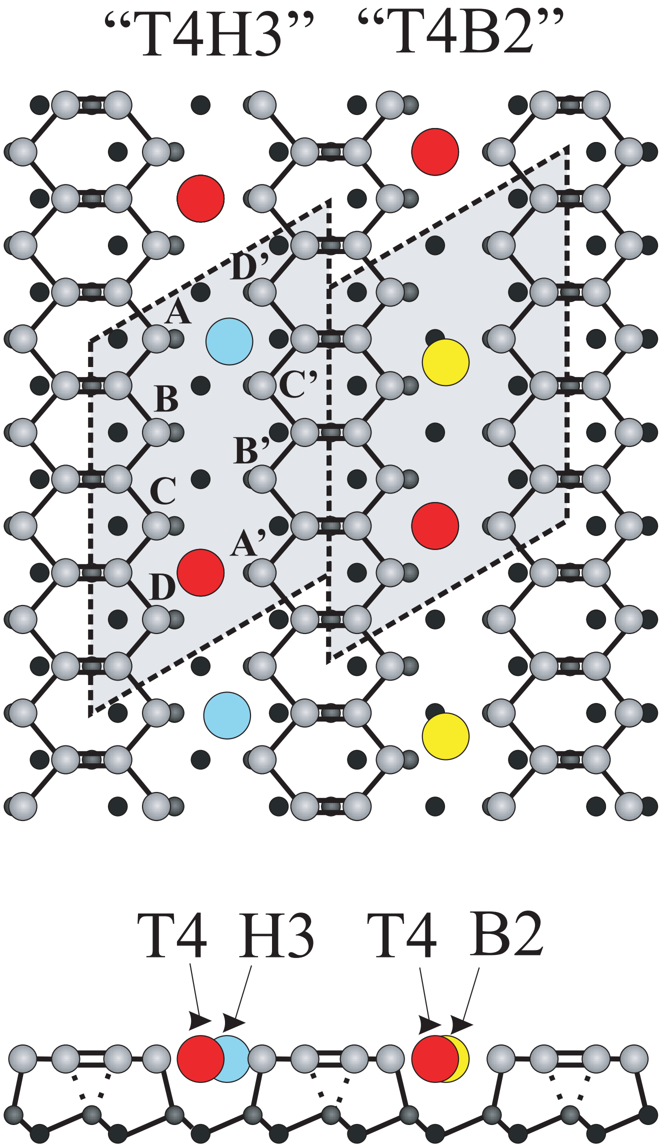

FIG. 7. (Color online) Atomic geometry of the Eu/Ge(111)-(3×4) HCC phase. The $T4H3$ and $T4B2$ configurations are shown. The surface unit cells are marked. The large circles are the metal atoms. See the text for detail.

(3×2) and -(3×4) phases, as suggested in Ref. 40. Another candidate for this site is the $B2$ one, as proposed for the Eu/Si(111)-(5×4) surface where 0.2 ML of Eu occupy $T4$ and 0.1 ML of Eu occupy $B2$.[30] Figure 7 shows both atomic configurations where half the Eu atoms are adsorbed on $T4$ and the other Eu atoms are adsorbed on either $H3$ (the "$T4H3$" model) or $B2$ (the "$T4B2$" model). Both of these models imply (*i*) the HCC arrangement of the Ge substrate, which is in good agreement with the filled-state and lower-bias empty-state STM images,[40] and (*ii*) one Eu atom per two (3×1) surface units, which is completely consistent with the semiconducting character of the Eu/Ge(111)-(3×2) surface and the divalent state of the Eu atoms in this reconstruction, as evidenced from the Eu 4f measurements (Sec. III B). The models also include linear Eu rows with a $\times 4$ periodicity and two alternative locations for the metal atoms, which agrees with the higher-bias empty-state STM images.[40] In the $T4B2$ configuration, however, the Eu atoms adsorbed on $T4$ and $B2$ are surrounded by different numbers of Ge atoms (i.e., by three and two Ge atoms, respectively). Therefore, such Eu atoms are not expected to have similar bonding configurations, as suggested in Sec. III B. Moreover, the $B2$ site is found to be less stable than the T4 and H3 sites in the HCC structure.[18,21,32] Thus, based on the above arguments, we do not consider further the $T4B2$ configuration of Fig. 7 for the Eu/Ge(111)-$(3\times 2)/(3\times 4)$ reconstruction.

In the $T4H3$ configuration, the numbers of Ge atoms that surround the Eu atoms adsorbed on $T4$ and $H3$ are identical. As seen in Fig. 7, the Eu atom at $T4$ is surrounded by the A', C, and D Ge atoms, and the Eu atom at $H3$ is surrounded by the A, C', and D' Ge atoms. The coordinations of A, C, and D atoms are very similar to those of the A', C', and D' atoms, respectively. It means that the bonding environments and charge states of the Eu atoms at $T4$ and $H3$ are quite similar, leading to a single multiplet component in the Eu 4f spectra in Fig. 3. In addition, we note that in the HCC structure, the energy difference of $H3$ and $T4$ is very small [e.g., 0.01 and 0.02 eV/atom for Ba (Refs. 18 and 21) and Ca,[32] respectively], and it is much lower as compared with the energy difference of $T4$ and $B2$ [e.g., 0.15 eV/atom for Ba/Si(111) (Refs. 18 and 21)]. Thus the $T4H3$ configuration is very possible, and therefore, we consider this configuration as the most plausible candidate for the atomic model of Eu/Ge(111)-$(3\times 2)/(3\times 4)$.

Next, we consider the Ge 3d results in the context of the $T4H3$ model. In the HCC structure, the outer atoms of the honeycomb chains have unsaturated dangling bonds, and therefore, these atoms can interact with the metal atoms. As a result of such interaction, the outer honeycomb-chain atoms are expected to gain more electronic charge than the bulk atoms due to the charge transfer from the metal atoms. Within the initial-state effects, it means that such surface atoms should have lower core-level binding energies than that of the bulk atoms. For the Eu/Ge(111)-(3×2) surface, the $S1$ and $S2$ components with negative SCLSs can be associated with the outer honeycomb-chain atoms, i.e., the A, A', B, B', C, C', D, and D' Ge atoms in Fig. 7. Taking into account the $S1/S2$ ratio and neglecting the diffraction effects, we assume that the number of Ge atoms, which are the origin of $S2$, is approximately three times larger than the number of Ge atoms, which are the origin of $S1$. The component $S1$ has the lowest BE meaning that the Ge atoms associated with the component gain more electron charge than the Ge atoms causing the component $S2$. In the $T4H3$ model, the D and D' Ge atoms are directly bonded to the Eu atoms at $T4$ and $H3$, respectively, and they can interact with the neighboring Eu atoms at $H3$ and $T4$, respectively. The A, C, A', and C' Ge atoms are also directly bonded to the neighboring Eu atoms at $H3$, $T4$, $T4$, and $H3$, respectively; however, the distances from these Ge atoms to their second neighboring Eu atoms, i.e., the ones at $T4$, $H3$, $H3$, and $T4$, respectively, are longer than the distance from D and D' to the Eu atoms at $H3$ and $T4$, respectively. Hence, the most plausible candidates for the atomic origin of $S1$ are the D and D' Ge atoms. Thus, taking into account that the number ratio of $(D+D'):(A+C+A'+C')$ is 1:3, we assign $S1$ to the D

and D' Ge atoms and $S2$ to the A, A', B, B', C, and C' Ge atoms.

The third Ge $3d$ surface component ($S3$) has a positive SCLS. The positively shifted component in Si $2p$ spectra of the Si(111)-(3×2) HCC reconstruction has been previously assigned to the inner honeycomb-chain atoms.[20,22,29,30] In both the Si and Ge HCC reconstructions, such atoms are suggested to form the Si═Si or Ge═Ge double bond and not to interact with the metal atoms directly. Consequently, the bonding configuration of such atoms is not expected to be sensitive to the adsorption sites of metal atoms in the channel between the honeycomb chains. In other words, the atomic arrangement of metal rows does not affect the charge state of the inner honeycomb-chain atoms. We therefore assign the present $S3$ component to the inner atoms of Ge honeycomb chains in the $T4H3$ model.

Finally we would like to remark on the $T4$ site in the HCC structure. In principle, the (3×4) periodicity on the Eu/Ge(111) surface can be arranged by means of a$\times$4 modulation along Eu chains in the $T4$ model of Fig. 1(b). For example, the (3×4) order would be constructed by placing every second Eu atom within the $T4$ (3×2) geometry to the position which is slightly shifted from the equilibrium $T4$ site. Note that the similar adsorbate-atom shift was earlier proposed in the (3×2) model with a coverage of 1/3 ML for the Ca/Si(111)-(3×2) (Ref. 15). Very recent total-energy calculations (Ref. 32), however, showed that such a metal-shifted configuration is not energetically stable, and it relaxes by moving the shifted metal atoms to the equilibrium $T4$ position in the fully optimized HCC structure.

V. CONCLUSIONS

In conclusion, we have examined the Eu-adsorbed Ge(111)-(3×2) surface at both 300 and 100 K by means of core-level photoelectron spectroscopy and LEED. The Eu $4f$ measurements reveal that this surface is semiconducting, and that the Eu atoms in the Ge(111)-(3×2) reconstruction are divalent. The final-state Eu $4f^6$ emission is found to be well reproduced by a single multiplet component; that is, all the Eu atoms have a similar bonding configuration on the surface. The analysis of Ge $3d$ core-level spectra investigated at various experimental conditions ($h\nu$, θ_e, and T) shows that the Ge $3d$ emission from the Eu/Ge(111)-(3×2) surface includes, in addition to the bulk component B, two surface-related components $S1$ and $S2$ shifted by ~0.6 and ~0.2 eV, respectively, to lower BE relative to B and one surface component $S3$ shifted by ~0.15 eV to higher BE relative to B. These results resemble the Si $2p$ fitting scheme for the divalent metal adsorbed Si(111)-(3×2) surfaces whose atomic structure is interpreted on the basis of the HCC structure with a 1/6 ML coverage of metal atoms adsorbed on $T4$ sites. However, the intensity ratios of the Ge $3d$ surface components for Eu/Ge(111)-(3×2) drastically differ from those of the metal-adsorbed Si(111)-(3×2) surfaces and cannot be explained with the $T4$ HCC model. We propose a modified structural model for the Eu/Ge(111)-(3×2)/(3×4) surface, where half of the Eu atoms are adsorbed on $T4$ and the other half on $H3$ (the $T4H3$ model). This model is shown to be consistent with the present photoemission results and the earlier STM observations. The atomic origins are proposed for $S1$, $S2$, and $S3$ within the $T4H3$ model.

ACKNOWLEDGMENTS

We are grateful to Mr. H. Ollila, T. Balasubramanian, and the MAX-lab staff for their assistance. The financial support by the Transnational Access to the Research Infrastructure Program (TARI) is acknowledged. This work has been supported in part by the Academy of Finland Grant No. 205766 (I. J. V.).

---

*Permanent address: A. F. Ioffe Physico-Technical Institute, Russian Academy of Sciences, 194021 St. Petersburg, Russian Federation. Electronic address: m.kuzmin@mail.ioffe.ru

[1] J. R. Ahn, N. D. Kim, S. S. Lee, K. D. Lee, B. D. Yu, D. Jeon, K. Kong, and J. W. Chung, Europhys. Lett. **57**, 859 (2002).

[2] P. Segovia, P. Purdie, M. Hengsberger, and Y. Baer, Nature (London) **402**, 504 (1999).

[3] H. W. Yeom, S. Takeda, E. Rotenberg, I. Matsuda, K. Horikoshi, J. Schaefer, C. M. Lee, S. D. Kevan, T. Ohta, T. Nagao, and S. Hasegawa, Phys. Rev. Lett. **82**, 4898 (1999).

[4] J. M. Carpinelli, H. H. Weitering, E. W. Plummer, and R. Stumpf, Nature (London) **381**, 398 (1996).

[5] R. Losio, K. N. Altmann, A. Kirakosian, J.-L. Lin, D. Y. Petrovykh, and F. J. Himpsel, Phys. Rev. Lett. **86**, 4632 (2001).

[6] H. H. Weitering, X. Shi, and S. C. Erwin, Phys. Rev. B **54**, 10585 (1996).

[7] Steven C. Erwin and Hanno H. Weitering, Phys. Rev. Lett. **81**, 2296 (1998).

[8] L. Lottermoser, E. Landemark, D.-M. Smilgies, M. Nielsen, R. Feidenhans'l, G. Falkenberg, R. L. Johnson, M. Gierer, A. P. Seitsonen, H. Kleine, H. Bludau, H. Over, S. K. Kim, and F. Jona, Phys. Rev. Lett. **80**, 3980 (1998).

[9] Myung-Ho Kang, Jin-Ho Kang, and Sukmin Jeong, Phys. Rev. B **58**, R13359 (1998).

[10] Shigehiko Hasegawa, Masakatsu Maruyama, Yoshitane Hirata, Daisuke Abe, and Hisao Nakashima, Surf. Sci. **405**, L503 (1998).

[11] A. A. Saranin, A. V. Zotov, V. G. Lifshits, J.-T. Ryu, O. Kubo, H. Tani, T. Harada, M. Katayama, and K. Oura, Phys. Rev. B **58**, 3545 (1998).

[12] M. Gurnett, J. B. Gustafsson, L. J. Holleboom, K. O. Magnusson, S. M. Widstrand, L. S. O. Johansson, M. K.-J. Johansson, and S. M. Gray, Phys. Rev. B **71**, 195408 (2005).

[13] O. Kubo, A. A. Saranin, A. V. Zotov, J.-T. Ryu, H. Tani, T. Harada, M. Katayama, V. G. Lifshits, and K. Oura, Surf. Sci. **415**, L415 (1998).

[14] A. A. Baski, S. C. Erwin, M. S. Turner, K. M. Jones, J. W. Dickinson, and J. A. Carlisle, Surf. Sci. **476**, 22 (2001).

[15] T. Sekiguchi, F. Shimokoshi, T. Nagao, and S. Hasegawa, Surf. Sci. **493**, 148 (2001).

[16] Y. K. Kim, J. W. Kim, H. S. Lee, Y. J. Kim, and H. W. Yeom, Phys. Rev. B **68**, 245312 (2003).

[17] Geunseop Lee, Suklyun Hong, Hanchul Kim, Dongsoo Shin, Ja-Yong Koo, Hyung-Ik Lee, and Dae Won Moon, Phys. Rev. Lett. **87**, 056104 (2001).

[18] Geunseop Lee, Suklyun Hong, Hanchul Kim, and Ja-Yong Koo, Phys. Rev. B **68**, 115314 (2003).

[19] T. Okuda, H. Ashima, H. Takeda, K.-S. An, A. Harasawa, and T. Kinoshita, Phys. Rev. B **64**, 165312 (2001).

[20] T. Okuda, K.-S. An, A. Harasawa, and T. Kinoshita, Phys. Rev. B **71**, 085317 (2005).

[21] Suklyun Hong, Geunseop Lee, and Hanchul Kim, J. Korean Phys. Soc. **47**, 100 (2005).

[22] Kazuyuki Sakamoto, Wakaba Takeyama, H. M. Zhang, and R. I. G. Uhrberg, Phys. Rev. B **66**, 165319 (2002).

[23] Kazuyuki Sakamoto, Wakaba Takeyama, H. M. Zhang, and R. I. G. Uhrberg, Surf. Sci. **532–535**, 628 (2003).

[24] Kazuyuki Sakamoto, H. M. Zhang, and R. I. G. Uhrberg, Phys. Rev. B **69**, 125321 (2004); Kazuyuki Sakamoto, A. Pick, and R. I. G. Uhrberg, *ibid.* **72**, 045310 (2005).

[25] C. Wigren, J. N. Andersen, R. Nyholm, U. O. Karlsson, J. Nogami, A. A. Baski, and C. F. Quate, Phys. Rev. B **47**, 9663 (1993); C. Wigren, J. N. Andersen, R. Nyholm, M. Göthelid, M. Hammar, C. Törnevik, and U. O. Karlsson, *ibid.* **48**, 11014 (1993).

[26] Frank Palmino, Eric Ehret, Louay Mansour, Jean-Claude Labrune, Geunseop Lee, Hanchul Kim, and Jean-Marc Themlin, Phys. Rev. B **67**, 195413 (2003).

[27] E. Ehret, F. Palmino, L. Mansour, E. Duverger, and J.-C. Labrune, Surf. Sci. **569**, 23 (2004).

[28] M. Kuzmin, R.-L. Vaara, P. Laukkanen, R. E. Perälä, and I. J. Väyrynen, Surf. Sci. **538**, 124 (2003); **549**, 183 (2004).

[29] M. Kuzmin, P. Laukkanen, R. E. Perälä, R.-L. Vaara, and I. J. Väyrynen, Phys. Rev. B **71**, 155334 (2005).

[30] Kazuyuki Sakamoto, A. Pick, and R. I. G. Uhrberg, Phys. Rev. B **72**, 195342 (2005).

[31] J. Schäfer, S. C. Erwin, M. Hansmann, Z. Song, E. Rotenberg, S. D. Kevan, C. S. Hellberg, and K. Horn, Phys. Rev. B **67**, 085411 (2003).

[32] R. H. Miwa, Phys. Rev. B **72**, 085325 (2005).

[33] J. W. Kim, S. Kim, J. M. Seo, S. Tanaka, and M. Kamada, J. Phys.: Condens. Matter **10**, 3731 (1998).

[34] M. Göthelid, S. Odasso, G. Le Lay, M. Björkqvist, E. Janin, U. O. Karlsson, and T. M. Grehk, Appl. Surf. Sci. **104&105**, 113 (1996).

[35] Geunseop Lee, Jonggeol Kim, I. Chizhov, H. Mai, and R. F. Willis, Phys. Rev. B **61**, 9921 (2000); Myonggeun Yoon, H. Mai, Geunseop Lee, and R. F. Willis, Surf. Sci. **463**, 183 (2000).

[36] Geunseop Lee, Jonggeol Kim, H. Mai, Ilya Chizhov, and R. F. Willis, J. Vac. Sci. Technol. A **18**, 1488 (2000).

[37] Geunseop Lee, H. Mai, and R. F. Willis, Phys. Rev. B **63**, 085323 (2001).

[38] Ji Young Lee and Myung-Ho Kang, Phys. Rev. B **66**, 233301 (2002).

[39] T. M. Grehk, M. Göthelid, M. Björkqvist, G. Le Lay, and U. O. Karlsson, Phys. Rev. B **61**, 4963 (2000).

[40] M. Kuzmin, P. Laukkanen, R. E. Perälä, and I. J. Väyrynen, Phys. Rev. B **73**, 125332 (2006).

[41] A. A. Saranin, V. G. Lifshits, K. V. Ignatovich, H. Bethge, R. Kayser, H. Goldbach, A. Klust, J. Wollschläger, and M. Henzler, Surf. Sci. **448**, 87 (2000).

[42] H. H. Weitering, Surf. Sci. **355**, L271 (1996).

[43] F. Gerken, J. Phys. F: Met. Phys. **13**, 703 (1983).

[44] W. D. Schneider, C. Laubschat, G. Kalkowski, J. Haase, and A. Puschmann, Phys. Rev. B **28**, 2017 (1983).

[45] N. Mårtensson, B. Reihl, W.-D. Schneider, V. Murgai, L. C. Gupta, and R. D. Parks, Phys. Rev. B **25**, 1446 (1982).

[46] M. Göthelid, T. M. Grehk, M. Hammar, U. O. Karlsson, and S. A. Flodström, Phys. Rev. B **48**, 2012 (1993).

[47] T. Okuda, H. Shigeoka, H. Daimon, S. Suga, T. Kinoshita, and A. Kakizaki, Surf. Sci. **321**, 105 (1994).